

AUTOMOTIVE COMPOSITE DRIVESHAFTS: INVESTIGATION OF THE DESIGN VARIABLES EFFECTS

M. A. Badie¹, A. Mahdi², A. R. Abutalib², E. J. Abdullah² and R. Yonus³

¹Department of Mechanical Engineering, Universiti Putra Malaysia, 43400, Serdang, Selangor, Malaysia

²Department of Aerospace Engineering, Universiti Putra Malaysia.

³Department of Chemical and Environmental Engineering, Universiti Putra Malaysia.

Email: badiesol@hotmail.com

ABSTRACT

Laminated composites, with their advantage of higher specific stiffness, gained substantiality in the field of torque carrying structures through many applications. Composite drive shafts offer the potential of lighter and longer life drive train with higher critical speed. In this study, finite element analysis performed to investigate the effects of fibers winding angle and layers stacking sequence on the critical speed, critical buckling torque and fatigue resistance. A configuration of a hybrid of one layer of carbon-epoxy (0°) and three layers of glass-epoxy (±45°, 90°) was used. The results show that, in changing carbon fibers winding angle from 0° to 90°, the loss in natural frequency is 44.5% and shifting from the best to the worst stacking sequence the DS loses 46.07% of its buckling strength, which gain the major concern over shear strength in DS design. The layers of ±45° angles are to be located far at inner side and that of cross-ply configuration located at top face with the 90° layer exposed to outside to increase the fatigue resistance, that the stacking sequence has an effect on fatigue properties.

Keywords: composite, driveshaft, LUSAS software, design variables, stacking sequence

INTRODUCTION

Drive shafts as power transmission tubing are used in many applications, including cooling towers, pumping sets, aerospace, trucks and automobiles. In metallic shaft design, knowing the torque and the allowable shear stress for the material, the size of the shaft's cross section can be determined. As the geometric parameter (polar moment of inertia of the cross-sectional area divided by the outer radius) equal to the torque divided by the allowable shear stress [1], there is unique value for the shaft inner radius when the outer radius is limited by the space under the car cabin. Metallic drive shaft has the limitations of weight, low critical speed and vibrational characteristics. Composite drive shafts have solved many automotive and industrial problems accompany the usage of the conventional metal ones because the performance is limited due to lower critical speed, weight, fatigue and vibration. Numerous solutions such as flywheels, harmonic dampers, vibration shock absorbers and multiple shafts with bearings, couplings, and heavy associated hardware have shown limited success in overcoming the problems [2].

When the length of steel drive shaft is beyond 1500 mm [3], it is manufactured in two pieces to increase the fundamental natural frequency, which is inversely proportional to the square length and proportional to the square root of specific modulus. The nature of composites with their higher specific modulus (modulus to density), which in carbon/epoxy exceed four times that of aluminum, enables the replacement of the two pieces metal shaft by one piece composite one which resonate at higher speed and so keeping higher margin of safety. A drive shaft of composites offers excellent vibration damping, cabin comfort, reduction of wear on drive train components and increasing tyres traction. In addition, the use of one piece torque tube reduces assembly time, inventory cost, maintenance, and part complexity. The first application of composite drive shaft to automotive was the one developed by Spicer U-joint divisions of Dana Corporation for the Ford econoline van models in 1985 [3].

Polymer matrix composites such as carbon/epoxy or glass/epoxy offer better fatigue characteristics as micro cracks in the resin not growth further like metals but terminated at the holes of fibers. Generally composites have less susceptibility to the effect of stress concentration such as those caused by notches and holes, than metals [4].

Filament winding process is used in the fabrication of composite drive shafts. In this process, fiber tows wetted with liquid resin are wound over a rotating male cylindrical mandrel. In this technique the winding angle, fiber tension, and resin content can be varied. Filament winding is relatively inexpensive, repetitive and accurate in fiber placement [5].

An efficient design of composite drive shaft could be achieved by selecting the proper variables, which can be identified for safe structure against failure and to meet the performance requirements. As the length and outer radius of drive shafts in automotive applications are limited due to spacing, the design variables include the inside radius, layers thickness, number of layers, fiber orientation angle and layers stacking sequence. In optimal design of the drive shaft these variables are constrained by the lateral natural frequency, torsional vibration, torsional strength and torsional buckling. In this study another constraint is added in term of torsional fatigue to be employed in the design of drive shafts by the selection of the stacking sequence.

1. DESIGN OPTIMIZATION OF COMPOSITE DRIVE SHAFT

The tailorability of elastic constants in composites provides numerous alternatives for the variables to meet the required stability and strength of a structure. First, fibers are selected to provide the best stiffness and strength beside cost consideration. It is the best selection, indeed, to use carbon fibers in all layers but due to their high prices a hybrid of layers of carbon-epoxy and E-glass-epoxy could be utilized. Since the fiber orientation angle that offers the maximum bending stiffness which leads to the maximum bending natural frequency is to place the fibers longitudinally at zero angle from the shaft axis, on the other hand, the angle of $\pm 45^\circ$ orientation realizes the maximum shear strength and 90° is the best for buckling strength. The main design goal is to achieve the minimum weight while adjusting the variables to meet a sufficient margin of safety, which is translated in a critical speed (natural frequency) higher than the operating speed, a critical torque higher than the ultimate transmitted torque and a nominal stress (the maximum at fiber direction) less than the allowable stress after applying any of the failure criteria like the maximum stress criteria.

Due to the physical geometry (larger radius) of the drive shafts used in the mentioned applications including automotive applications, the shear strength which specify the load carrying capacity, is of minor design importance since the failure mode is dominated by buckling, therefore the main design factors are the bending natural frequency and the torsional buckling strength, which are functions of the longitudinal and hoop bending stiffness, respectively. The variable of the laminate thickness has a big effect on the buckling strength and slight effect on bending natural frequency. A discrete variable optimization algorithm could be employed for optimization of ply thickness and orientation. Rangaswamy et al. [6] used Genetic Algorithm and Rastogi [3] used GENESIS/I-DEAS optimizers for the optimization of variables in the design of drive shaft in automotive applications. Darlow and Creonte [7] employed the general-purpose package OPT, version 3.2 in optimizing the lay-up of a graphite-epoxy composite drive shaft for helicopter tail rotor.

2. DESIGN PROCEDURE

The material properties of the drive shaft analyzed through the classical lamination theory. This theory, which deals with the linear elastic response of laminated composite, incorporates the assumption of Kirchhoff-love for bending and stretching of thin plates beside the assumption that each layer is in state of plane stress [8]. From the properties of the composite materials at fibers direction, the first step is the construction the reduced stiffness matrix. The expressions of the reduced stiffness coefficients Q_{ij} in terms of engineering constants are as follows:

$$\begin{aligned} Q_{11} &= \frac{E_1}{1 - \nu_{12}\nu_{21}} & Q_{22} &= \frac{E_2}{1 - \nu_{12}\nu_{21}} & Q_{66} &= G_{12} \\ Q_{12} &= \frac{\nu_{12} E_2}{1 - \nu_{12}\nu_{21}} & \nu_{21} &= \frac{E_2}{E_1} \nu_{12} \end{aligned} \quad (1)$$

The second step is to construct the extensional stiffness matrix $[A]$. This matrix is the summation of the products of the transformed reduced stiffness matrix $[\bar{Q}]$ of each layer and the thickness of this layer as:

$$[A] = \sum_{K=1}^N [\bar{Q}]^K (z_K - z_{K-1}) \quad (2)$$

The A matrix is in (Pa.m) and the thickness of each ply is calculated in reference of their coordinate location in the laminate. The A matrix is used to calculate E_x and E_h , which are the average moduli in the axial and hoop directions, respectively from:

$$E_x = \frac{1}{t} \left[A_{11} - \frac{A_{12}^2}{A_{22}} \right] \quad E_h = \frac{1}{t} \left[A_{22} - \frac{A_{12}^2}{A_{11}} \right] \quad (3)$$

2.1 BUCKLING TORQUE

Since the drive shaft is long, thin and hollow, there is a possibility for it to buckle. The expression of the critical buckling torque for thin-walled orthotropic tube is given as [9]

$$T_{cr} = (2\pi r^2 t)(0.272) [E_x E_h^3]^{1/4} \left(\frac{t}{r} \right)^{3/2} \quad (4)$$

Where r , is the mean radius and t is the total thickness. It is obvious that the stiffness modulus at hoop direction (E_h) plays the big role in increasing the buckling resistance. The factor of safety is the ratio of the buckling torque to the ultimate torque.

2.2 LATERAL BENDING NATURAL FREQUENCY

The drive shaft is designed to have a critical speed (60 times the frequency), that is high enough to exceed the rotational speed. If both are become coincident a large amplitude vibration (whirling) occurs. The drive shaft is idealized as simply supported at its ends or pinned-pinned beam. The lowest natural frequency expression is given as [10], [11]

$$f_n = \frac{\pi}{2} \sqrt{\frac{g E_x I}{W L^4}} \quad (5)$$

where g is the gravity acceleration, W is the weight per unit length, L is the length and I is the moment of inertia, which is, in the thin-walled tube equal to

$$I_x = \frac{\pi}{4} (r_o^4 - r_i^4) \approx \pi r^3 t \quad (6)$$

where r is the mean radius and t is the wall thickness. To increase the natural frequency, carbon fibers are required to be oriented along the axial direction.

2.3 LOAD CARRYING CAPACITY

The composite drive shaft is designed to carry the torque without failure. The torsional strength or the torque at which the shaft fail, is directly related to the laminate shear strength through

$$T_s = 2 \pi r_m^2 t \tau_l \quad (7)$$

where T_s is the failure torque, τ_l is the in-plane shear strength of the laminate, r_m is the mean radius and t is the thickness. The same formula is used in laboratory after a torsion tube test to determine the shear modulus and shear strength of materials. Since the laminate is assumed to be failed at the failure of the first ply, the maximum stress failure criterion could be used after finding the in-plane stresses at every ply to specify a factor of safety for torque transmission capacity. The first step is to construct the transverse of the extensional stiffness matrix $[A]$ and after solving for the overall strains, the stresses in each layer can be examined by transforming these stresses to the direction of fibers at each layer. The layers of fiber direction $\pm 45^\circ$ are of special concern since they have the substantial contribution to the load carrying. The A^{-1} matrix multiplied by the through thickness resultant forces matrix N gives the resultant strain as follow:

$$\{\varepsilon\} = A^{-1} \begin{Bmatrix} N_x \\ N_y \\ N_{xy} \end{Bmatrix} = A^{-1} \begin{Bmatrix} 0 \\ 0 \\ N_{xy} \end{Bmatrix} \quad N_{xy} = \frac{T}{2\pi r^2} \quad (8)$$

The axial force $N_x = 0$, the centrifugal force N_y is neglected and N_{xy} is the resultant shear force. The torque T is the peak torque if the design involves fatigue considerations [12]. The resultant strains transformed to the fiber direction by multiplying these strain matrices by the transformation matrix. Then the plane stresses could be obtained.

$$\begin{Bmatrix} \varepsilon_1 \\ \varepsilon_2 \\ \gamma_{12} \end{Bmatrix} = \begin{bmatrix} m^2 & n^2 & mn \\ n^2 & m^2 & -mn \\ -2mn & 2mn & m^2 - n^2 \end{bmatrix} \begin{Bmatrix} \varepsilon_x \\ \varepsilon_h \\ \gamma_{xh} \end{Bmatrix} \quad (9) \quad \begin{Bmatrix} \sigma_1 \\ \sigma_2 \\ \tau_{12} \end{Bmatrix} = \begin{bmatrix} Q_{11} & Q_{12} & 0 \\ Q_{12} & Q_{22} & 0 \\ 0 & 0 & Q_{33} \end{bmatrix} \begin{Bmatrix} \varepsilon_1 \\ \varepsilon_2 \\ \gamma_{12} \end{Bmatrix} \quad (10)$$

2.4 TORSIONAL FREQUENCY

Another concept is the torsional frequency. This frequency is directly related to the torsional stiffness (T/ϕ), where ϕ is the angle of twist and T is the applied torque. The frequency of torsional vibration can be presented as:

$$f_t = \frac{1}{2\pi} \sqrt{\frac{K}{I_m}} \quad (11)$$

K , being the torsional spring rate, is equal to the torsional stiffness. I_m is the mass moment of inertia at propeller. For a given geometry of specific drive shaft, the torsional stiffness is directly related to the modulus of rigidity (G_{xy}) as follows [2]:

$$K = \frac{T}{\phi} = \frac{G_{xy} J}{L} \quad (12)$$

J , is the polar moment of inertia and L is the length. The shear modulus can be tailored to its maximum value by orienting the fibers at an angle equal to 45 degrees. In some applications like racing cars, less torsional stiffness is required [2]. The shear modulus could be directly obtained when the extensional stiffness matrix $[A]$ constructed, by dividing the shear stiffness component A_{66} by the total thickness of the drive shaft as follow:

$$G_{xy} = \frac{A_{66}}{t} \quad (13)$$

The practical application of torsional vibration systems are engines. These engines have damping (source of dissipation of energy) in the crankshafts (hysteresis damping) and in inertias (damping in torsional vibration dampers and in propellers). Since damping present is normally small in magnitude, for determining the natural frequency it is ignored [13].

3. FINITE ELEMENT ANALYSIS OF DRIVE SHAFT

Finite element models of the drive shaft were generated and analyzed using LUSAS version 13.5-7 commercial software. Three dimensional model was developed and typical meshing generated by using three-dimensional thick shell element (QTS8). This degenerate continuum element is capable of modeling warped configurations, accounts for varying thicknesses and enables for anisotropic and composite material properties to be defined. Since it is quadrilateral, it uses an assumed strain field to define transverse shear which ensures that the element does not lock when it is thin and the quadratic elements like this one can accommodate generally curved geometry [14]. Cylindrical local coordinate dataset has been defined to align the material direction of the composite lay-up and to apply ends supports and loading.

Eigenvalue linear buckling analysis was performed to define the critical buckling torque. The output from this analysis is a factor multiplied by the applied load to find the critical buckling load. The linear analysis is considered satisfactory in comparison with nonlinear analysis due to the fact that cylindrical shells under torsion load experienced less sensitivity to imperfection [15], mentioning that, in this study, the position of buckling region in the axial length of the shaft is recognized to be shifted towards the end of the shaft when a nonlinear analysis performed. Modal analysis is a technique used to analyze structures dominated by global displacement like in vibration problems. It was used to define the natural frequency of the drive shaft. The eigen vectors resulted from the eigenvalue analysis are the modes of buckling deformation and bending natural frequency as presented in Figures (1) and (2).

A composite drive shaft design example presented by [12] was taken as a reference in constructing a model for all analysis. In this example, a shaft of length 1730 mm, mean radius 50.8 mm and lay-up consist of three layers of ($\pm 45^\circ$, 90°) glass-epoxy and 0° carbon-epoxy layer were used. The ultimate torque is 2030 Nm and the minimum bending natural frequency is 90 Hz. The material properties are as in Table 1.

Table 1: Material Properties [12]

Material	E_{11} (GPa)	E_{22} (GPa)	G_{12} (GPa)	Ultimate Strength (MPa)	Weight Density (Kg/m ³)
E-glass-epoxy	40.3	6.21	3.07	827	1910
Carbon-epoxy	126.9	11.0	6.6	1170	1610

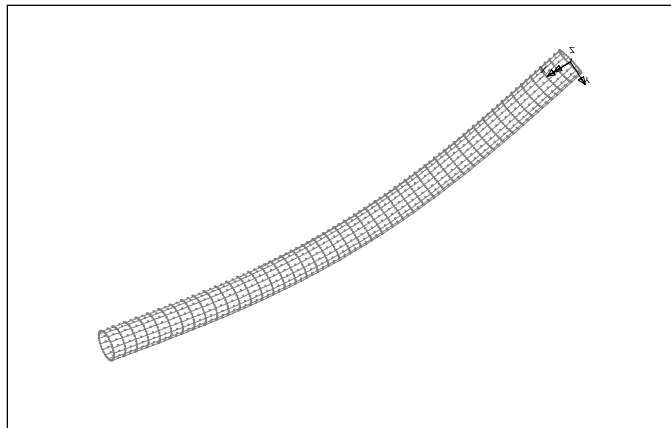


Figure 1: The first mode of natural frequency

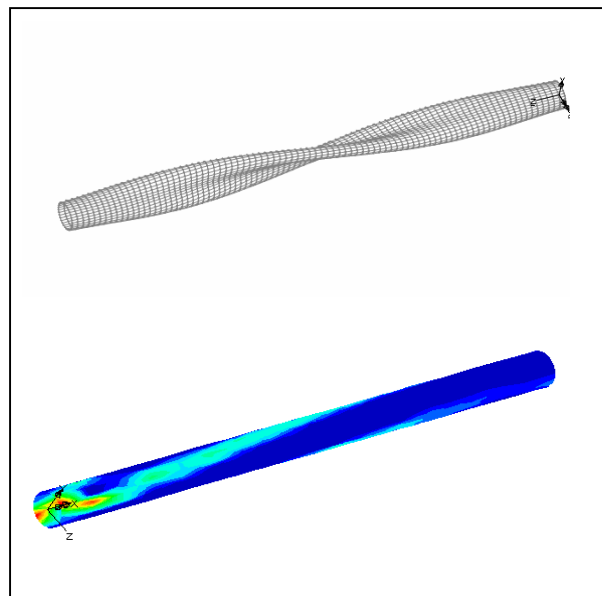


Figure 2: The first mode shape of buckling and the corresponding contour of maximum shear stress

4. EFFECTS OF FIBERS ANGLE AND STACKING SEQUENCE

The fibers orientation angle has a big effect on the natural frequency of the drive shaft. A configuration consists of four layers stacked as $[+45^{\circ}_{\text{glass}} / -45^{\circ}_{\text{glass}} / 0^{\circ}_{\text{carbon}} / 90^{\circ}_{\text{glass}}]$ was analyzed and it is clear that from Figure 3, the fibers must be oriented at zero degree to increase the natural frequency by increasing the modulus of elasticity in the longitudinal direction of the shaft. This explain why the carbon fibers, with their high modulus saved to be oriented at zero angle. The drive shaft loses 44.5% of its natural frequency when the carbon fibers oriented in the hoop direction at 90° instead of 0° . The cost factor plays a roll in selecting only one layer of carbon/epoxy. The stacking sequence has no effect on the natural frequency since there is no load applied in defining the natural frequency.

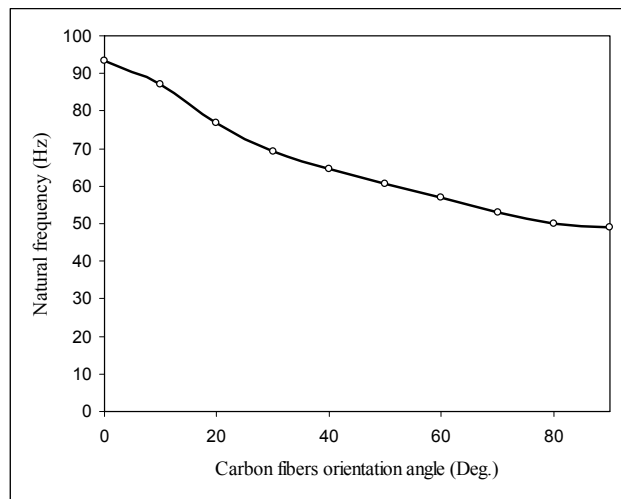


Figure 3: The effect of changing the carbon fiber orientation angle in a hybrid drive shaft of stacking $[\pm 45^\circ_{\text{glass}}/0^\circ_{\text{carbon}}/90^\circ_{\text{glass}}]$ on the natural frequency

With the intension of perceiving the behavior of composite tubes under different physical dimension, it is found that the decrease of fiber orientation angle to increase the natural frequency is not monotonic; the analysis conducted on comparatively thin composite tubes, shows that the behavior of the thinner tube is different and the critical speed or the natural frequency not increases regularly as the orientation angle approaches the value of zero. From Figure 4, three models of the same material (carbon/epoxy) and different thicknesses were constructed. It is found that the critical speeds for all models are the same when the fibers of all layers oriented at 38 to 90 degrees. However, as the thickness increases the range from 38-90 angles increases. The best fiber orientation angle for maximum buckling strength is 90° . At this angle the fibers oriented in the hoop direction and therefore the modulus (E_h) increased.

Figure 5 presents the effect of changing the fiber orientation angles of the two glass/epoxy layers on the buckling torque. As shown in Figure 6 the behavior of the graphs is not the same in changing the angles of different layers and it is clear that, when changing the angles of the 3rd or the 4th layer or both of them, the critical buckling torque of the drive shaft is not regularly affected by the fiber orientation angles. Hence, the interrelation of the laminate layers must be investigated prior to the final design.

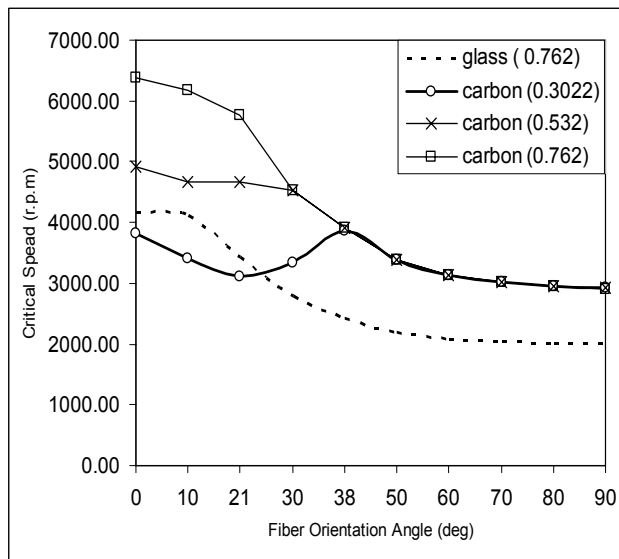


Figure 4: Comparisons between the critical speeds of composite tubes having four layers and stacking of $[\theta]_4$

Note: 1- Glass and carbon are abbreviation of glass/epoxy and carbon/epoxy
 2- Figures in parentheses indicate total thickness in millimeters

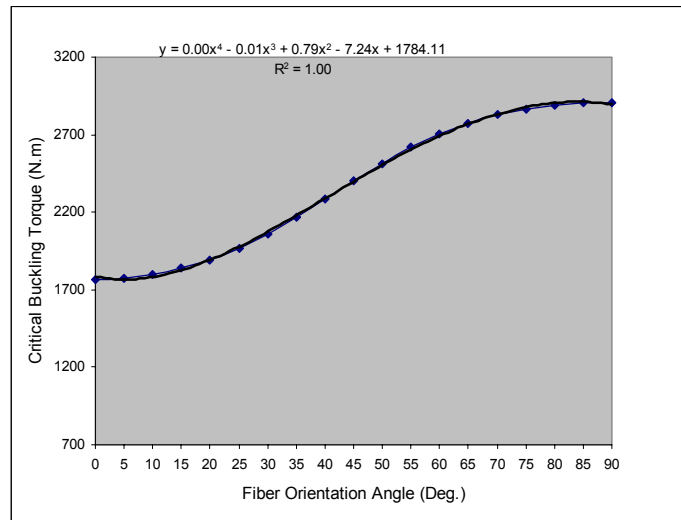


Figure 5: Effect of fiber orientation angle on buckling torque by changing the first two layers of stacking [$\pm 45^\circ_{\text{glass}} / 0^\circ_{\text{carbon}} / 90^\circ_{\text{glass}}$]

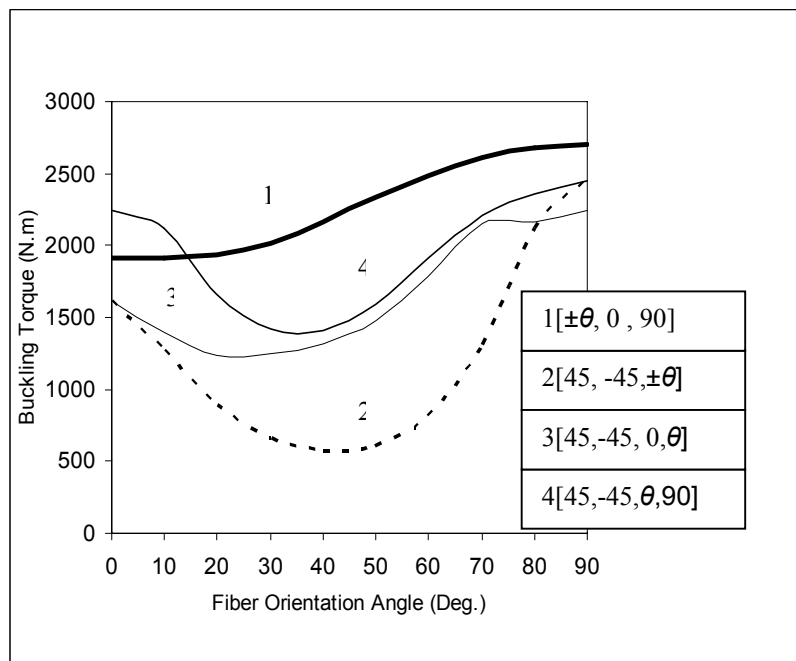


Figure 6: Effect of fiber orientation angle of different layers on buckling torque of a drive shaft having stacking of [$\pm 45^\circ_{\text{glass}} / 0^\circ_{\text{carbon}} / 90^\circ_{\text{glass}}$]

The stacking sequence of the layers has an effect on the buckling strength. As the $[A]$ matrix is independent of the stacking sequence, both $[B]$ and $[D]$ matrices are dependent. The drive shaft buckled when its bending stiffness along the hoop direction can't support the applied torsion load. This normal bending stiffness is correspondent to the component D_{22} of the bending stiffness matrix $[D]$. Therefore, the value of D_{22} specifies the resistance of the drive shaft to deflect radially or to (buckle).

The stiffness matrices could be defined in fast procedure by using one of the available software for analyzing the composite laminates such as The Laminator [16], which was used in this study. Figure 6 presents the effect of

stacking sequence on the buckling strength and it is concluded that the best stacking sequence is $[45^\circ/-45^\circ/0^\circ/90^\circ]$ with a normal bending stiffness equal to $58.8 \text{ Pa}\cdot\text{m}^3$ and the worst stacking is $[0^\circ/90^\circ/-45^\circ/45^\circ]$ with a normal bending stiffness component equal to $36.23 \text{ Pa}\cdot\text{m}^3$. The best stacking offers a buckling torque of 2303.1 Nm and the worst stacking offers a torque of 1242 with a loss in buckling resistance capability equal to 46.07%.

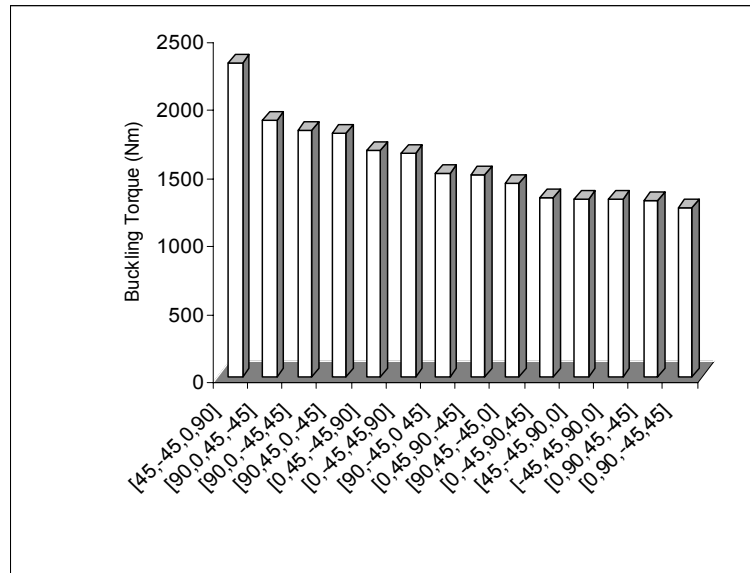


Figure 7: Effect of stacking sequence on buckling torque

5. FATIGUE STRENGTH

It is known from previous studies that the torsional fatigue exhibit linear behavior on the S-N plot scaled as log-log. The torsional fatigue strength of $\pm 45^\circ$ carbon/epoxy specimen is approximately 3.7-3.8 times higher than that of the 0° specimens at an equivalent number of cycles [17].

In this study the effect of layers stacking sequence has been investigated. It is founded that, neither the maximum stress at the axial direction nor the maximum shear stress give different effects of different stacking sequence, when they used to plot the S-N diagram. Only the average mid-surface plane shear stress is the stress that gives different fatigue cycles to failure for different stacking sequence. The worst zone of the drive shaft from fatigue resistance side of view is the gripping zone.

The fatigue resistance for any structure can be evaluated from the S-N diagram by the inclination and location of the plotted lines compared to each others. The less inclination and top position is the best. Figure 7 presents comparison between S-N diagrams of different stacking sequences for layers of the same thicknesses, materials and fiber orientation angles. It can be concluded that, in designing for fatigue consideration, the layers of $\pm 45^\circ$ fiber orientation must kept close to each other having a location near to the inner surface with the cross-ply angles layers located exposed to outside with the seniority of the 90° layer at the outer face location. For buckling strength, the layers of $\pm 45^\circ$ angles are not a matter if located inside or outside as in $[45, -45, 0, 90]$ and $[90, 0, -45, 45]$ configurations, because their hoop normal bending stiffness term D_{22} have the same magnitude.

Ranking due both fatigue and buckling strengths for different stacking sequences is presented in table 7. Due to this ranking, the stacking configuration of $[\pm 45, 0, 90]$ fulfills both the best fatigue and buckling resistance characteristics because it satisfy the requirements of the angle-and cross-ply locations, in addition it have the maximum value of the normal bending stiffness component D_{22} .

Table 2: Comparisons between fatigue and buckling Strengths for different stacking configurations of [$\pm 45^\circ_{\text{glass}}/0^\circ_{\text{carbon}}/90^\circ_{\text{glass}}$]

Configuration	Ranking due to Fatigue Strength	Ranking due to Buckling Strength
[45,-45,0,90]	1 st	1 st
[45,-45,90,0]	2 nd	3 rd
[0,90,-45,45]	3 rd	4 th
[90,0,-45,45]	4 th	2 nd

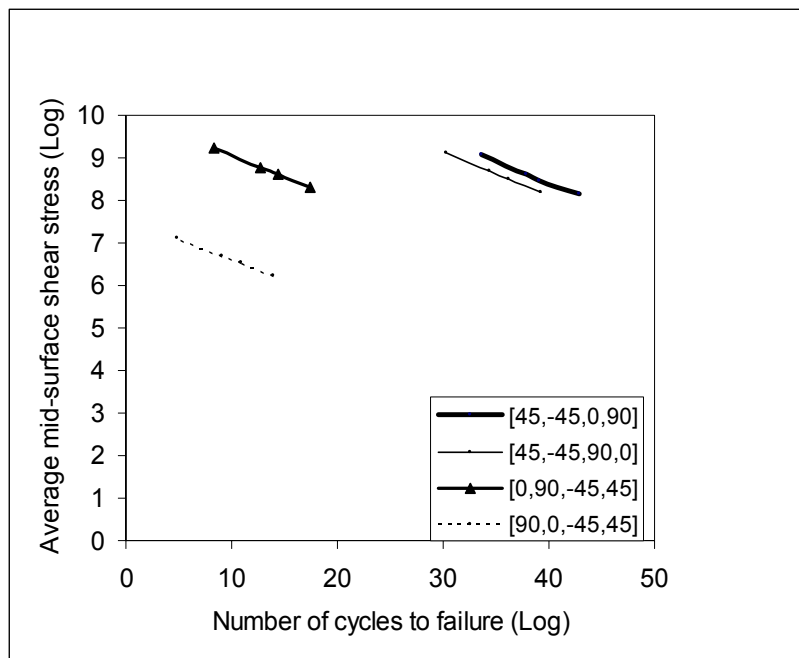


Figure 7: Torsional S-N diagrams for selected stacking sequence configurations

6. CONCLUSION

The present finite element analysis of the design variables provide an insight of their effects on the drive shaft critical mechanical characteristics and fatigue resistance. A model of hybridized layers was generated incorporating both carbon-epoxy and glass-epoxy. The buckling, which dominates the failure mode, have a value not increases regularly with increasing the winding angle. At the worst layers stacking sequence the shaft loses 46.07% of its buckling strength realized at the best stacking sequence. On the other hand, the stacking sequence has an obvious effect on the fatigue resistance of the drive shaft.

REFERENCES

- [1] Hibbeler, R. C. (2003), *Mechanics of Materials*, SI Edition, Prentice Hall, Upper Saddle River, New Jersey.
- [2] Leslie, J. C., Troung, L., Blank, B. and Frick, G., (1996), Composite driveshafts: technology and experience, SAE Special Publications 1203, pp. 43-52, Paper No. 962209.
- [3] Rastogi, N. (2004), Design of composite driveshafts for automotive applications, SAE, Technical Paper Series, 2004-01-0485.
- [4] Jones, R. M., (1999), *Mechanics of Composite Materials*, 2nd edition, Tailor Francis, Philadelphia.
- [5] Mallick, P. K. (1997), *Composite engineering handbook*, Marcel Dekker, New York.
- [6] Rangaswamy, T., Vijayarangan, S., Chandrashekar, R. A., Venkatesh, T. V. and Anantharaman, K. (2004), Optimal design and analysis of automotive composite drive shaft, International Symposium of Research Students on Materials Science and Engineering, India.
- [7] Darlow, M. S. and Creonte, J. (1995), Optimal design of composite helicopter power transmission shafts with axially varying fibre lay-up, *Journal of the American Helicopter Society* **40** (2): 50-56.
- [8] Herakovich, C. T., (1998), *Mechanics of fibrous composites*, John Wily & Sons, New York.
- [9] Column Research Committee of Japan, ed., (1971) *Handbook of structural stability*, Corona Publishing, Tokyo.
- [10] Timoshenko, S., Young, D. H. and Weaver, W., (1959), *Vibration problems in engineering*, 4th Edition, John Wiley and Sons, New York.
- [11] Thomson, W. T. (1998), *Theory of vibration with applications*, 5th ed., Prentice Hall, Upper Saddle River, New Jersey.
- [12] Swanson, S. R. (1997), *Introduction to design and analysis with advanced composite materials*, Prentice Hall, Upper Saddle River, New Jersey.
- [13] Ramamurti, V. (1998), *Computer-aided mechanical design and analysis*, 3rd Edition, McGraw-Hill, New York.
- [14] LUSAS, User's manual, version 13.7-5.
- [15] Simitzes, G. J., Shaw, D., and Sheinman, I. (1985), Imperfection sensitivity of laminated cylindrical shells in torsion and axial compression, *Journal of Composite Structure*, **4**: 335-60.
- [16] The Laminator software, version 3.6.
- [17] Mallick, P. K. (1993), *Fiber-reinforced composites: materials, manufacturing, and design*, 2nd edition, Marcel Dekker, New York.